Title: Tracing root-felt sodium concentrations under different transpiration rates and salinity levels

Authors: Adi Perelman[1], Helena Jorda[2], Jan Vanderborght[2, 3], and Naftali Lazarovitch[1*]

Affiliations: [1]French Associates Institute for Agriculture and Biotechnology of Drylands, Jacob Blaustein Institutes for Desert Research, Ben-Gurion University of the Negev, Midreshet Ben-Gurion, Israel

[2]Department of Earth and Environmental Sciences, Faculty of Bioscience Engineering, KU Leuven, Leuven, Belgium

[3]Institute of Bio- and Geoscience, Agrosphere Institute, IBG-3, Forschungszentrum Jülich GmbH
Jülich, Germany

*Corresponding author current address: French Associates Institute for Agriculture and Biotechnology of Drylands, Jacob Blaustein Institutes for Desert Research, Ben-Gurion University of the Negev, Midreshet Ben-Gurion, Israel, email: lazarovi@bgu.ac.il

Abstract

Aims: (1) Monitoring 'root-felt' salinity by using rhizoslides as a non-invasive method, (2) Studying how transpiration rate, salinity in irrigation water, and root water uptake affect sodium distribution around single roots, (3) Interpreting experimental results by using simulations with a 3-D root system architecture model coupled with water flow and solute transport models.

Methods: Tomato plants were grown on rhizoslides under various salinity levels and two transpiration rates: high and low. Daily root images were processed with GIMP and incorporated into a 3-D numerical model. The experiments were simulated with R-SWMS, a 3-dimensional numerical model that simulates water flow and solute transport in soil, into the root and inside root systems.

Results: Both experimental and simulation results displayed higher root-felt sodium concentrations compared with the bulk concentrations, and larger accumulation at higher transpiration rate. The simulations illustrated that the root-felt to bulk concentration ratio changed during the experiment depending both on the irrigation water salinity and transpiration rate.

Conclusions: Changes in sodium concentrations with transpiration rates are most likely caused by root water uptake and ion exclusion. Simulation results indicate that root-scale process models are required to link root system architecture, environmental, and soil conditions with root-felt salinities.

Key words: root water uptake, process model, roots, saline irrigation

Abbreviations

HT: high transpiration rate

LT: low transpiration rate

dist: distance from the root interface

DDW: double distilled water

EC: electrical conductivity

Introduction

Salinity stress is one of the main factors limiting crop growth and productivity, especially in arid and semi-arid areas (Yang et al. 2009). It has been estimated that 20% of total cultivated and 33% of irrigated agricultural lands worldwide are afflicted by salinity. Moreover, salinized areas are increasing at an annual rate of 10%. The common assumption today, according to the Maas and Hoffman model (1977), is that when salinity in the root zone increases beyond a certain threshold, it will result in yield reduction at a fixed rate. This model is considered to be a macroscopic model relating plant responses to averaged root zone salinity and averaged meteorological conditions during an entire growing season (Groenveld et al. 2013). Many enviromental and economical studies (e.g. Feddes et al. 2001; Houk et al. 2006) used the Maas and Hoffman model as a base for decision making. The model considers neither the effect of transient evaporative demand on the reduction rate of the plant water uptake [which is generally associated with plant growth and crop yield, (Ben-Gal et al. 2003)] due to salinity, nor its effect on salt accumulation at the root-soil interfaces. Since the conditions at the root-soil interface define the impact of salinity on plants, the 'root-felt' salinity should be monitored. When salts cannot enter freely with the water flow into the roots, they accumulate at the soil-root interface. We aim to show the effect of transpiration demand on the actual root-soil interface salt concentrations and their difference from the bulk root zone salt concentrations. This will enable to evaluate and describe dynamic changes in the plant response to salinity and will support crop management decisions considering time variable evaporative demand, leaching fractions or irrigation salinities.

The term salinity refers to the presence of various ions in soil and water at concentrations that are damaging to many agricultural crops. Most common solutes related to salinity are the dissociated cations Na^+, K^+, Ca^{2+}, and Mg^{2+}; and the anions Cl^-, SO_4^{2-}, NO^{3-}, HCO_3^- and CO_3^{2-} (Hillel 2000). Beyond the general effects of salinity on crops growth and productivity (like osmotic stress), there can also be specific ion effects (Lauchli and Grattan 2007; Grieve et al. 2011). Na^+ is considered to be one of the major ions contributing to salinity stress, due to its negative effects on crops and soils: Na^+ is not essential to plant's growth, moreover high Na^+

concentrations interfere with plant uptake of essential nutrients such as K^+ or Ca^{2+}, alongside its harmful effect on the soil's physical properties (Hillel 2000). Therefore, this research was focused on investigating Na^+ accumulation at the root-soil interface. This approach does not consider other elements in the system, Na^+ interactions with other ions in the solution (e.g. competitions on absorption) and how such interactions affect plant mineral uptake and ion accumulation. However, it does allow relatively simple and rapid measurements, assuming that Na^+ is the main cause of damage of salinity stress.

Roots in their natural environment can be reached and measured only by using special equipment and procedures (Polomsky and Kuhn 2002). Thus, in root research today, there is a growing need for developing new methods that will enable to track root growth and architecture and to obtain accurate measurements of water and solute distributions, especially when studying the root-soil interface. Studies aiming at quantifying root growth in soils are often restricted by the lack of suitable methods for continuous, non-destructive measurements (Kuchenbuch and Ingram 2002). A solution to these problems can be using a paper-based growth system such as rhizoslides. This kind of paper can be used not only for germination testing but also to assess root traits, as the paper is easy to handle, can be kept free from pathogens and enables the management of a large number of replicates on a limited space. Moreover, the access to the root system is fairly simple (Le Marié et al. 2014). Rhizoslides have some limitations as they are not actual soil and they only allow for root growth in 2D (the paper has negligible thickness). Nevertheless, rhizoslides are porous media where solute gradients can develop and are relatively easy to measure. For the first time, rhizoslides were used to trace Na^+ concentrations around single roots in response to various salinity levels and transpiration demands.

Transpiration rate is suspected to be a factor influencing salt accumulation around roots and thereby increasing the root felt concentration. This will impact the whole plant sensitivity to the salinity level of the irrigation water. Water moves through the soil to the plant root and from the root to the transpiring leaves along pressure gradients (Denmead and Shaw 1962), therefore, any factor affecting transpiration will ultimately impact root water uptake. Water

storage in most crops (herbaceous plants) is minimal (Wohlfahrt et al. 2006), and the amount of water that these plants can lose by transpiration is even lower when compared to the amount of water that is transpired. Therefore, root water uptake responds almost immediately to transpiration. Additionally, there is a correlation between the amount of water transpired and mineral uptake from the soil (Barber 1962), so it is possible to assume that Na^+ movement toward the root will also be affected by transpiration rate and/or root water uptake.

Sinha and Singh (1976) observed differences in Na^+ accumulation around corn and wheat roots, depending on different transpiration rates. They also reported higher Na^+ concentrations around the roots compared with the bulk soil. Riley and Barber (1970) reported that salt accumulation increased with higher salt concentration in the soil solution and higher transpiration rate. These observations were made at the whole root system level and not at a single root level.

With time, the paradigm of simulation models has been extended to include interactions between plants and their environment, resulting in models that can be accepted as research tools in biology (Mech and Prusinkiewicz 1996; Passot et al. 2018). Inclusion of these interactions implies that the environmental conditions can be spatially resolved so that the simulated conditions represent the real conditions that control or influence the processes in the soil-plant-atmosphere continuum. It also implies that fluxes in the environment are consistently coupled with fluxes in the plant. In the context of root water uptake from saline soils, this suggests that water fluxes and solute transport are simulated in the coupled soil-plant system and that fluxes towards and within single root segments are resolved (Schröder et al. 2014; Jorda et al. 2017). Such approach allows considering salt accumulation at the root-soil interface (instead of bulk soil salinity) and its effect on water potential differences between the root and the soil and on root water uptake.

The objectives of this study were (i) to investigate the effect of transpiration rate and salinity level on salt accumulation at the root-soil interface using paper rhizoslides and (ii) to interpret the observed salt accumulation with simulated salt accumulation by a numerical model that solves the water flow and solute transport towards and in a growing root system.

Using this comparison, the experimentally observed data can be linked to processes in the system that support their interpretation.

Materials and methods

Experiments were conducted to achieve the following: (1) to develop a new experimental system and fit it to the research needs and (2) to examine the effects of irrigation salinity levels and transpiration rates on Na^+ distribution around a single root. The experimental system is based on rhizoslides: 460 X 580 X 0.6 mm glass fiber filter sheets (Fipa MN GF-4, fibers diameter ≤ 3.5 µm & ≥ 10 µm in length), MACHEREY-NAGEL GmbH and Co. KG, Germany) on which plants are grown under different transpiration regimes and using different irrigation water salinities (Fig 1). Before running experiments with plants, the rhizoslide water retention curve was determined from pressure chamber and sand box experiments. The van Genuchten water retention function (van Genuchten 1980) was fitted to water content data measured at different pressures (Fig 2).

Different salinity levels, corresponding to different electrical conductivities (EC) of the irrigation water, were achieved by adding NaCl to double distilled water (DDW), for the calibration experiment. Approximately: EC = 1 dS m^{-1} ~ 0.55 g/L NaCl ~ 150 ppm of Na^+. For the plant experiments, NaCl was added to NPK fertilizer 20:20:20 solution (1 g/L, background EC = 1 dS m^{-1}) until the desired EC was reached. EC of the solutions was measured using a conductivity meter (CON 510, EUTECH instruments, Singapore).

To measure Na^+ concentrations at different locations along the sheets, discs of 0.7 cm diameter were cut out using a hole-puncher. Cutout discs were placed in tubes containing 1 mL DDW and shaken for two hours to extract the solutes from the sheet. The volume of the disc is around 0.02 mL, thus the water volume in the disc can be neglected compared to the water volume of the added water, so that concentrations in the extract can be translated to concentrations per bulk volume of paper. The salinity of the solution was expressed in terms of the Na^+ concentration that was measured in the extract using a Na^+ specific electrode (B-722 LAQUAtwin Compact Sodium Ion Meter, Horiba, Japan).

To evaluate the feasibility of this approach, we tested the method in a calibration experiment. The sheets were dipped in different solutions in the range of EC = 1-6 dS m^{-1} and a calibration curve was made between Na^+ concentrations in the applied solutions and Na^+ concentrations in the extracts from the cutout discs (Fig 3). Because the consistency of the water saturated paper was very low, it was not possible to cut out disks from the wet paper. The paper was therefore dried before taking the cutouts. The slope of the curve corresponded quite well with the ratio of the water volume in the disk to the added water volume (0.02 mL/ 1 mL). However, due to variations in both the thickness of the paper, its porosity and water content, and non-uniform drying of the paper which led to a lateral redistribution of Na^+, individual points may deviate from the calibration line. In the experiments with plants grown on the paper, the paper was not fully saturated when the discs were punctured. Since the water content was not known, the concentration in the paper that was derived from the disc extracts using the inverted calibration relation, represents in fact the Na^+ concentration in the paper when DDW would be added to the paper until it was fully saturated with water. When we assume that the water content in the paper does not vary with distance from the roots or with the transpiration rate of the plant, then the concentrations measured directly in the extracts can be used to compare concentrations at different distances from the root or different transpiration rates. Simulation results showed that the maximum difference in volumetric water content at different transpiration rates and at different distances from the roots was 0.026 and 0.011, respectively. Therefore, we considered our assumption valid.

Tomato seeds were sown in growth substrate, in a growth room with the following conditions: 24/18 °C (day/night), 12 hours of light, relative humidity (RH) 65%. About 3 weeks after germination, the root system was cut out close to the collar and after washing, the plants were placed in DDW for 3-4 days, until new roots emerged. Then, plants were placed on rhizoslides, inside A4 office plastic bags (for support and evaporation prevention). The plants stayed covered to minimize transpiration for couple of days to encourage root establishment on the sheets and were irrigated with DDW to prevent algae or fungi growth. After roots were established, water was applied through a small cut at the bottom of the plastic bag, keeping the pipette from touching the slide itself, to avoid washing off solutes (Fig 1). Thus, water

183 movement in the sheets was due to capillary rise and root water uptake only. Because
184 rhizoslides are a closed system, water loss occurred only through transpiration, so the irrigation
185 volume was approximately the same as the volume transpired by the plants. The plants were
186 irrigated for two weeks; this period is enough to allow the root system to develop on the
187 rhizoslide without the roots becoming overcrowded, which would hinder Na^+ sampling. After
188 two weeks, samples were taken at three distances in perpendicular direction from the root: (1)
189 -0.35-0.35 cm, (2) 0.35-1.05 cm and (3) 1.05-1.75 cm. This sampling method was performed at
190 three different locations. The discs were cut out when the sheets were almost dry.

191 Plants were divided into two transpiration rate treatments: (1) High rate (HT) – plants
192 grown in open air; this rate will be considered as 100% transpiration; (2) Low rate (LT) – plants
193 were kept covered with a transparent cover (increase in air humidity and reduction in air
194 movement) during the growth period. This cover was not completely sealed to prevent CO_2
195 depletion. Transpiration rate of the LT, which was calculated from the amount of applied water,
196 was 60% of the HT. A second treatment factor was the salinity of the irrigation water and two
197 sets of irrigation water salinities were generated: (a) treatments of EC = 2, 4, and 6 dS m^{-1}, and
198 (b) treatments of EC = 1.5, 2, 2.5, 3, 3.5, and 4 dSm^{-1}. The number of plants per salinity-
199 transpiration treatments combination (n) was n = 7 for subset (a) and n = 4 for subset (b). From
200 each sheet, nine samples were taken so that all together 378 discs were sampled from subset
201 (a) and 432 discs from subset (b). Plants and leaves fresh biomass was measured from two
202 treatments combination, EC 1.5 and 4 dSm^{-1} under HT and LT, using an analytical scale.

203 In the last experiment, established plants were placed in a net-house for 15 days, with the
204 following conditions: 32/20 °C (day/night), 13 hours of light, RH 50%. 60 tomato plants were
205 divided to HT and LT, combined with two irrigation salinities of 1.5 and 4 dSm^{-1}, and 15 plants in
206 each treatment combination. Out of 15 plants in each salinity-transpiration treatment
207 combination, 6 plants were sampled. From each sheet, nine samples were taken so that all
208 together 216 discs were sampled. Samples were taken from different positions along the
209 rhizoslide (top, middle and bottom) and at growing distance from the root, as mentioned

above. Data were used to observe and simulate differences in Na^+ accumulation at different positions along the rhizoslides.

Data analysis and image processing

To facilitate the discussion and comparison between experimental and simulation results (see further), we calculated concentration ratios of Na^+ concentrations in the extracts among distances

$$Na^+ \ concentration \ ratio \ \left(\frac{dist\ 1}{dist\ 3}\right)[\%] = 100\frac{[Na^+]_1}{[Na^+]_3} \quad (1)$$

where $[Na^+]_1$ represents the Na^+ concentrations at the closest distance to the root and $[Na^+]_3$ represents the Na^+ concentrations at the farthest distance from the root.

For determining significant difference between treatments, data were analyzed using JMP statistical analysis program (JMP®, Version 10. SAS Institute Inc., Cary, NC, 1989-2007). Means were compared using 'Student t test' or 'Tukey test', depending on the amount of comparisons (see supplementary material).

Photos of the root systems of tomato plants were taken on a daily base, using a Nikon camera (Digital SLR Camera D3200, Nikon Japan), from establishment of the plants on the rhizoslides until Na^+ measurements for a period of 15 days. Root systems of all the plants, in each treatment combination, were manually drawn on the photos using GIMP 2.0 (GNU Image Manipulation Program, {www.gimp.org}).

Model simulations

Rhizoslide experiments were simulated with R-SWMS (Javaux et al. 2008). R-SWMS is a 3-dimensional numerical model that simulates water flow and solute transport in soil, into the root and inside detailed root architectures. Water flow into the root is a function of radial root conductance and the gradient in water potential between the root xylem and soil-root interface. In order to consider the effect of Na^+ accumulated at the root surface on radial flow, the osmotic potential was added to the matric potential at both soil-root interface and xylem:

$$q_r = L_r\left((h_s - h_x) + \sigma\left(h_{o,s} - h_{o,x}\right)\right) \quad (2)$$

where q_r is the radial root flow (L T^{-1}), Lr is the radial root conductance (L T^{-1}), h_s is the soil-root interface matric potential (L), h_x is the xylem matric potential (L), $h_{o,s}$ is the soil-root interface osmotic potential (L), $h_{o,x}$ is the xylem osmotic potential (L) and σ is the reflection coefficient.

The reflection coefficient σ can vary between zero and one. It represents the effectiveness of the membrane complex of the root surface to selectively allow water flow but not salt transport across the membrane. When σ is 1, no solute is allowed to cross the membrane (total exclusion). On the contrary, when σ is 0, all solutes can enter the root with the water radial flux, and therefore osmotic potentials do not drive water flow across the membrane. Simulations were conducted under the assumption of salt exclusion since tomatoes are thought to be salt excluders.

Osmotic potentials were calculated from solute concentrations according to:

$$h_o = \beta c \quad (3)$$

where β was -50 µmol^{-1} cm^4, as in Schröder et al. (2014) and c (µmol cm^{-3}) is the solute concentration.

To run the simulations, different data were collected from the rhizoslide experiments. The obtained segmented images (abovementioned) were run through Root System Analyzer software (Leitner et al. 2014) and were used to produce input files with root architecture information. Data on plant transpiration were gathered from recorded irrigation volumes assuming that there were no evaporation losses from the rhizoslides. Soil water retention parameters found in Figure 2 were used to parameterize the soil domain. A saturated hydraulic conductivity, K_s of 700 cm d^{-1} was assumed to run the simulations. This is a common value used to parameterize sand texture (Carsel and Parrish 1988; Schaap et al. 2001), which we considered similar to the texture of the paper.

Simulations were performed on six different root systems (Fig 4) under two transpiration rates (low = 3 cm^3 day^{-1}, and high = 5 cm^3 day^{-1}). Transpiration demand was applied at the root

collar as a sinusoidal boundary condition from 6 AM to 6 PM, with highest demand during midday and no demand between 6 PM and 6 AM. Constant irrigation was applied from the bottom of the domain with different EC levels (2, 4 and 6 dS m^{-1}). Root development was included in the simulations by updating the root system with time according to the images obtained from the rhizoslides experiments. The root system hydraulic parameters were L_r (radial conductivity) = 1.728 10^{-4} cm s^{-1} cm^{-1} and K_x (xylem conductivity) = 4.32 10^{-2} cm^4 s^{-1} cm^{-1}. These parameters were obtained from Doussan et al. (1998), where they studied maize roots. Since the root system was cut out and regrew again at the beginning of the experiment, the maximal age difference between roots was only about two weeks. We therefore did not consider parameterization as a function of root age.

Virtual salt concentration measurements were taken every 12 hours and at numerous sampling points along each root system (Fig 4). The sampling points were selected by choosing root segments that were sufficiently apart from other roots so that a distinction could be observed between the soil-root interface and the near bulk.

Na^+ concentrations were calculated in three different ways. First, we calculated Na^+ concentrations at distances 1, 2 and 3 at the sampling locations (Fig 4) by averaging concentrations in an area that corresponded to that in the experimental setup. Second, we calculated root-soil interface Na^+ concentrations. This concentration was obtained by averaging the Na^+ concentration in all elements containing root segments for the whole root system. Finally, we calculated the weighted average root-felt concentration for the whole root system using the following equation:

$$C_{root\ felt} = \frac{\sum_{i=1}^{n} C_i q_{r,i}}{\sum_{i=1}^{n} q_{r,i}} \quad (4)$$

where i is the root segment, n is the number of root segments, C_i is the concentration at the root-soil interface of root segment i, and $q_{r,i}$ is the radial flow of root segment i. Root-felt concentrations were compared to bulk concentrations. Bulk concentrations were calculated by averaging the concentrations in the domain until the depth reached by the root system.

Results

A significant difference in leaves biomass was observed between low and high transpiration rates at EC = 4 dS m^{-1}, but not at EC = 1.5 dS m^{-1}. When comparing the whole plant biomass, there were significant differences between the plant biomass under HT and LT at each salinity level but not between the different salinity levels (Table 1). This indicated that plants did not suffer from osmotic stress caused by high salinities.

Na^+ concentration in the rhizoslide experiments showed an increase with increasing irrigation salinity levels and proximity to the root. At each measurement location, Na^+ concentrations were mostly found to be higher under HT than LT (Fig 5). Na^+ concentrations around the root were significantly higher compared with bulk concentrations, even at a very short distance of 0.5 cm from the root interface. Ratios between Na^+ concentrations at the closest distance to the root (dist 1) and the farthest (dist 3), at each treatment combination (salinity level X transpiration rate), were calculated and are shown in Figure 6. The ratios are always above 100%, indicating that Na^+ accumulation occurred near the roots. In half of the cases, under LT there is a higher ratio of accumulation compared with HT, but the absolute values of Na^+ concentration in LT are lower in comparison to HT.

As in the experimental results, the simulations results did not show a decrease in transpiration rate due to osmotic stress for both low and high transpiration rate scenarios. Moreover, larger Na^+ concentration and accumulation at the root-soil interface were simulated in HT scenarios compared to LT. A previous simulation study by Jorda et al. (2017) also observed larger accumulation of salt with increasing transpiration rate.

Figure 7 shows relative Na^+ concentration distributions (relative to the Na^+ concentration in the irrigation water) in the domain at different times for simulations performed on plant 1 under low and high transpiration and 4 dS m^{-1} in the irrigation water. In the beginning of the simulation, water flowed upwards by capillary flow and consequently Na^+ was transported towards the top of the profile. Na^+ started accumulating around root segments for both low and high transpiration demand scenarios. After 12 days, it was observed that under LT demand, Na^+ accumulation at the root surface mainly occurred at roots located in the middle upper part of the profile, where most water was taken up (Fig 7 d-e and Fig 8a). In contrast, Na^+

316 concentration at the soil-root interface was lower than in the bulk in the lower half of the
317 profile. This phenomenon occurred for all simulations under low transpiration demand. To
318 explain this behavior, we plotted the water sink distribution per depth for one of the
319 simulations (plant 1 and 4 dS m^{-1}) in Figure 8. Both under HT and LT conditions, root water
320 uptake took place mainly in the upper part of the profile where salinity was lower. However,
321 during night, plants under LT took up water from the top profile and released it to lower parts
322 of the profile where the total water potential was lower due to the higher salt concentration.
323 Such redistribution of water to lower parts of the profile was also simulated during daytime (Fig
324 8a). This led to a less saline rhizosphere with respect to the bulk soil in the lowest part of the
325 root zone of the LT treatments. In contrast, under HT, Na^+ accumulation occurred throughout
326 the root system and water redistribution was not sufficient to invert solute gradients. In the HT
327 treatments, the accumulation of salts in the upper part of the root zone lowered the total
328 water potential to such an extent that it remained lower than in the deeper part of the root
329 zone so that at the end of the simulation period, redistribution at night occurred from the
330 deeper part of the profile to the upper part. The accumulation of salts in the upper part of the
331 root zone for HT treatments also led the plant to take up water from lower parts of the root
332 zone during day, whereas root water uptake remained mainly in the upper part for LT
333 treatments.

334 For HT demand scenarios, a higher Na^+ concentration was simulated at the closest distance
335 to the root than at the furthest distance during the entire simulation period (Fig 9 d-f). At LT
336 demand, however, we observed that from day 10 until day 14 there was an inversion in the
337 gradient or no difference in Na^+ concentration among distances (Fig 9 a-c). As mentioned above,
338 when the root system grew to the bottom of the profile, we could observe two differentiated
339 zones: the upper area where the bulk salinity was lower than in the deeper zone and where the
340 root took up water and Na^+ accumulated at the root surface; and the lower area where water
341 was released during night leading to a rhizosphere that was less saline than the bulk. Since we
342 virtually sampled simulated gradients all over the root system, we obtained average values that
343 indicate no difference among distances. In addition, we simulated large variability in solute
344 concentration values per distance and treatment. In Figure 9, the standard error of the mean

(SEM) that was calculated from 21 samples (in agreement with the 3 samples that were taken for each of the 7 plants in the experiment with the first set of irrigation salinities, subset a) was plotted. We divided the standard deviation of the simulated concentrations at a certain distance by the square root of 21 to calculate the SEM. The simulation results offer a good estimate of the standard deviation of the solute concentration at different distances observed in the rhizoslide setup. The obtained SEM is a useful tool to assess whether, given the expected variability of solute concentration in the rhizoslide setup, the number of samples was enough to observe significant differences among distances. According to the simulation results, 21 was a sufficient number of samples to observe significant differences between distances to the root under HT treatment. However, under LT this number of samples seemed insufficient. The simulation results showed that until about 6-7 days, there is significant difference among distances, especially between distances 1 and 2 compared to 3. However, once water redistribution starts (see Fig 8c), these differences become non-significant.

In Figure 9, we compared Na^+ concentration at dist 1 (dark blue line) with the average Na^+ concentration at the root-surface for all root segments (red line). Under HT treatments, we underestimated root-soil interface concentration since roots that take up most water at the top center of the profile are not accessible for sampling (see Figs 4 and 8a) and we observed the highest accumulation of salts in that area (see Fig 7j). Similarly, root-soil interface concentration under LT treatment was underestimated during the beginning of the simulations time. This shows the impact of sampling uncertainty and the bias that is caused by restricting the sample location to roots that are accessible.

For both low and high transpiration demand, the simulation results demonstrated a decreasing Na^+ accumulation ratio with time (Fig 10). At the beginning of the simulation, Na^+ concentration at the closest distance to the root (dist 1) was 200% larger than at the furthest distance (dist 3) from the root for both transpiration rates. However, by the end of the simulation the percentage decreased to 125% and 170% for low and high transpiration rates, respectively. These results are within the range of values observed in the experimental results (Fig 6). The decreasing ratio is a consequence of the increasing root density with time in

373 combination with a transpiration rate that remained constant over time, which caused a
374 reduction of root water uptake per length of root segment with time and led to lower
375 accumulation of salt at the root surface (Jorda et al. 2017).

376 We also observed that the effect of transpiration rate on the simulated Na^+ distribution
377 changed with time and differed between distances (Fig 11). In the beginning of the simulation,
378 Na^+ concentration at the different distances from the root was about 110% to 150% larger at
379 high than at low transpiration. After 10 days, this difference became larger, showing that the
380 accumulation of Na^+ in the profile at HT was nearly 600% higher than at LT for an EC = 6 dS m^{-1}.
381 Towards the end of the simulation, these ratios decreased to 180-280 %. These dynamics were
382 highly influenced by the slower arrival of saline water near the roots under LT with respect to
383 HT simulations. The ratios of simulated Na^+ concentrations under HT and LT were considerably
384 higher than the observed ratios in the experimental setup (see Fig 6). This could be due to
385 differences in root architecture between the LT and HT experiments, which were not
386 considered in the simulation scenarios. Total plant mass (and hence root mass) was higher in
387 the HT experiments so that the water uptake per unit length for HT compared to LT did not
388 increase that much in the experiments compared to the simulations. Finally, during the first half
389 of the simulation, the ratios for different distances were similar among salinity treatments.
390 However, after 8 days, we can observe that transpiration rate had a stronger effect on the
391 closest distance to the root, where the ratio in concentration between high and low rate was
392 from 1.2 to 1.5-fold higher than at the larger distances.

393 In addition, simulation results under HT revealed higher Na^+ concentration at dist 1 from
394 the root at sampling points located at the top profile of the rhizoslides compared with those at
395 the middle and bottom parts (see Figs 7 and 12). To verify these findings, we examined the
396 experimental Na^+ concentrations taken at different positions (see methods) along the rhizoslide
397 and the largest Na^+ concentration was found at the top profile as well. We compared Na^+
398 concentrations from LT in the net-house experiment to simulated concentrations under HT for
399 which average daily transpirations were similar (Fig 12).

In the experimental setup, to allow the roots to establish on the papers and prevent them from experiencing stress, plants were initially irrigated with non-saline water. Therefore, once the transpiration and salinity treatments started, there were two processes happening at the same time: saline water replacing non-saline water in the papers, and salt accumulation at the root surface. The simulations allow us to understand the effect of these two processes. Simulations with initial salinity in the capillary paper equal to the salinity of the irrigation water indicated that the ratio of Na^+ concentration of distance 1 to 3 was larger than in simulations with no initial salinity in the rhizoslide. However, towards the end of the simulation the ratio tended to similar values. The ratio between HT and LT was lower when the paper was initially saline. This is caused by the much faster accumulation of salinity in the HT than in the LT scenarios when no salinity is present in the paper initially. Nevertheless, we still simulated a higher accumulation of Na^+ under HT than at LT.

Finally, Figure 13 presents the comparison between root-felt and dist 1 concentrations. Concentrations at dist 1 showed close correlation to root-felt concentrations for HT treatments. However, concentrations at dist 1 tended to be higher than root-felt concentrations under LT. Higher concentrations at the root surface than root-felt concentrations can be explained by the fact that, on the one hand, roots generate higher salinities around the root surface due to water uptake and salt exclusion. This leads to higher concentrations at the root surface than in the bulk (Fig 9). However, when there is a spatial gradient of salinity in the root zone, root water uptake can shift towards regions where salt concentration is lower (and the absolute value of the osmotic potential is lower, see for instance Fig 8b). This leads in most cases to a lower root-felt salinity than the salinity at the root surface.

Discussion

Results from Na^+ accumulation measurements support evidences found in former studies (Riley and Barber 1970; Sinha and Singh 1976), but provide finer resolution, as previous work was done in the general root zone. Hamza and Aylmore (1992) also reported increased Na^+ accumulation at the interface of a single root under high transpiration rate, nevertheless, they did not measure changes in Na^+ concentration as a function of distance from the root. These

findings stress the importance of measurement location. Hence, to gain a full understanding of Na^+ accumulation processes around roots, measuring Na^+ concentrations in the general root zone or from soil extracts might be insufficient. Measuring Na^+ concentration from soil extracts provides average values, at specific time points within a whole growing season. Even methods such as suction cups supply average values from relatively large soil volumes and do not provide data at a single root scale. Changes in Na^+ concentrations with transpiration rate are probably caused by root water uptake. Therefore, root water uptake distribution along the root system will influence the differences in solute concentration within the root zone.

Results from transpiration rate experiments support the hypothesis that under low transpiration rate and low plant water uptake, less Na^+ accumulates around the root. This means that plants growing under low transpiration demands might survive at higher salinity levels of irrigation, compared with plants growing under high transpiration demands. Transpiration rate is affected by different factors such as air temperature and relative humidity, CO_2 levels and light intensity among others. Low transpiration might cause reduction in plant size and crop yield by reducing nutrients uptake in general (Adams 1980) and specifically the transport of calcium (Stebbins and Dewey 1972). In this study, the leaves and whole plant biomass were compared between transpiration rates at two salinity levels: EC = 1.5 and 4 dS m^{-1}. A significant difference was observed between HT and LT under saline irrigation, but not under non-saline irrigation. When analyzing separately the effect of salinity and transpiration rate, transpiration had a significant effect on leaves biomass, while salinity did not. This means that during the time of the experiment, salinity stress did not develop or was not strong enough to affect the plant's growth. On the other hand, reduced transpiration rate led to a lower photosynthesis rate and to smaller plants. Plants biomass was measured only from two salinity levels, EC = 1.5 and 4 dS m^{-1}. If we had sampled plants from higher salinity levels or had grown the plants for a longer period, we might have seen the salinity effect on the plant's growth as well.

Vapor pressure deficit (VDP) has also been found to affect plants salinity tolerance: plants were relatively tolerant to salinity during periods of low VPD and relatively sensitive during

periods of high transpiration demand (Groenveld et al. 2013). However, our data did not show stronger sensitivity of plants to salinity under higher transpiration rates, as plant mass under high transpiration was even higher for the high salinity than for the low salinity treatment. The higher accumulation of Na^+ near the roots under high transpiration indicates however that the conditions that generate salinity stress may be reached earlier under high than under low transpiration rates.

The simulation results showed a strong correspondence with the experimental results and allowed us to observe phenomena that were not examined in the experiment itself. For instance, we noticed water redistribution under both HT and LT conditions in the simulations. Redistribution phenomena have been studied with a special focus on "hydraulic lift", where roots take up water from the wetter deep soil and release it to the upper drier soil. However, studies such as that of Burgess et al. (2001) observed water movement from top to bottom in trees. Redistribution processes are thought to occur whenever a potential gradient exists across soil layers and the soil reaches a potential threshold that causes water to flow from roots to soil (Warren et al. 2007). In our study, water redistribution decreased the solute gradients developed around single roots by transporting water from more to less saline root zones. Such behavior might help the plant manage salt accumulation at the root surface and delay the onset of stress.

Conclusions

In roots research, most measurements are usually taken from the general root zone and not at a single root level or near the root-soil interface. In this study, a recently developed setup, called rhizoslides, was used to quantify solute accumulation at the root surface at the scale of single roots. In addition, we investigated the effect of transpiration rate on the "root-felt" Na^+ concentration, a parameter that is neglected in most water flow and solute transport models. Tomato plants were grown on rhizoslides setups for 15 days under two transpiration rates and different irrigation water salinities. The results of these experiments indicate that Na^+ concentration around the root is higher than in the bulk soil, even at a short distance as 0.5 cm. Na^+ accumulation at the root-soil interface increased with transpiration rate, supporting

484 evidences from previous studies. The main disadvantage of using rhizoslides is that their
485 properties are different from agricultural soils. This difference may affect how fast and how
486 much Na^+ accumulates around the root. In addition, rhizoslides are a 2D system, which might
487 influence the root systems' growth and uptake, compared to roots growing surrounded by a 3D
488 medium. Despite these limitations, unlike other soilless methods for growing roots such
489 hydroponics and aeroponics, rhizoslides enable measuring Na^+ concentration at the root
490 surface and at different distances from it. In addition, they also allow for temporal and spatial
491 monitoring of root growth. To overcome the shortcomings of the rhizoslides setup, we used a
492 detailed-architectural root model coupled to a water flow and solute transport model. The
493 models enabled us to simulate conditions that are hard to reproduce or observe in real
494 experiments, such as a large number of treatments. They also provide insight in the dynamic
495 evolution of variables that are measured destructively in most experimental setups. In this
496 study, simulation results support the experimental work by putting the measurements into
497 temporal and spatial perspective. Simulation results indicated that the temporal dynamics of
498 salt accumulation at the root-soil interface were highly influenced by transpiration rate, total
499 root length and root water uptake distribution along the root system. For instance, Na^+
500 accumulation at the root surface decreased with increasing root length. This information can be
501 relevant to plant breeders who can, for example, engineer rootstocks with larger root length to
502 make plants more tolerant to salinity. Simulations also pointed out that water redistribution
503 processes might be relevant under certain conditions. To improve models' accuracy, they must
504 be compared against experimental data before they can become part of a physiological
505 experiment tools box. Such a toolbox could then be used to transfer information and insights
506 that are obtained from lab scale experiments to the field and use it for adjusting irrigation
507 scheduling and salinity and optimizing the use of resources. It is therefore important to have a
508 cross-talk between models and experiments, as they should rely on each other.

509

Acknowledgement

This research was supported by a Grant from the GIF, the German-Israeli Foundation for Scientific Research and Development and by the Israel Ministry of Agriculture and Rural Development (Eugene Kandel Knowledge Centers) as part of the “Root of the Matter: The root zone knowledge center for leveraging modern agriculture.”

Bibliography

Adams P (1980) Nutrient uptake by cucumbers from recirculating solutions. Acta Hort 119–126

Barber SA (1962) A diffusion and mass-flow concept of soil nutrient availability. Soil Sci. 93:39–49

Ben-Gal A, Karlberg L, Jansson PE, Shani U (2003) Temporal robustness of linear relationships between production and transpiration. Plant Soil 251:211–218

Burgess SSO, Adams MA, Turner NC, et al (2001) Tree roots: Conduits for deep recharge of soil water. Oecologia 158–165

Denmead OT, Shaw RH (1962) Availability of Soil Water to Plants as Affected by Soil Moisture Content and Meteorological Conditions1. Agron J 54:385

Doussan C, Page L, Vercambre G (1998) Modelling of the Hydraulic Architecture of Root Systems : An Integrated Approach to Water Absorption-Model Description. Ann Bot 81:213–223

Feddes RA, Hoff H, Bruen M, et al (2001) Modeling root water uptake in hydrological and climate models. Bull Am Meteorol Soc 82:2797–2809

Grieve CM, Grattan SR, Maas E V. (2011) Plant Salt Tolerance. In: Wesley W. Wallender PD, P.E.; Kenneth K.Tanji S. (eds) Agricultural Salinity Assessment and Management, second. American Society of Civil Engineers, Reston, VA, pp 405–459

Groenveld T, Ben-Gal A, Yermiyahu U, Lazarovitch N (2013) Weather determined relative sensitivity of plants to salinity: quantification and simulation. Vadose Zo J 12:9 pp.

Hamza M, Aylmore L (1992) Soil solute concentration and water uptake by single iupin and radish plant roots 1. Water extraction and solute accumulation. Plant Soil 145:187–196

Hillel D (2000) Salinity Management for Sustainable Irrigation Integrating Science, Environment, and Economics. The International Bank for Reconstruction and Development/THE WORLD BANK

Houk E, Frasier M, Schuck E (2006) The agricultural impacts of irrigation induced waterlogging and soil salinity in the Arkansas Basin. Agric Water Manag 85:175–183

542 Javaux, Mathieu, Schröder, Tom, Vanderborght, Jan, Vereecken H (2008) Use of a Three-
543 Dimensional Detailed Modeling Approach for Predicting Root Water Uptake. Vadose Zo J
544 7:1079

545 Jorda H, Perelman A, Lazarovitch N, Vanderborght J (2018) Exploring Osmotic Stress and
546 Differences between Soil–Root Interface and Bulk Salinities. Vadose Zo J 17:0

547 Kuchenbuch RO, Ingram KT (2002) Image analysis for non-destructive and non-invasive
548 quantification of root growth and soil water content in rhizotrons. J Plant Nutr Soil Sci
549 165:573–581

550 Lauchli A, Grattan S. (2007) Plant growth and development under salinity stress. In: Jenks MA,
551 Hasegawa PM, Jain SM (eds) Advances in Molecular Breeding Toward Drought and Salt
552 Tolerant Crops. pp 1–32

553 Le Marié C, Kirchgessner N, Marschall D, et al (2014) Rhizoslides: paper-based growth system
554 for non-destructive, high throughput phenotyping of root development by means of image
555 analysis. Plant Methods 10:13

556 Leitner D, Felderer B, Vontobel P, Schnepf A (2014) Recovering Root System Traits Using Image
557 Analysis Exemplified by Two-Dimensional Neutron Radiography Images of Lupine. PLANT
558 Physiol 164:24–35. doi: 10.1104/pp.113.227892

559 Maas EV, Hoffman GJ (1977) Crop salt tolerance: evaluation of existing data. Water Irrig. Proc
560 Intern Salin. 187–198

561 Mech R, Prusinkiewicz P (1996) Visual models of plants interacting with their environment. Proc
562 23rd Annu Conf Comput Graph Interact Tech 96:397–410

563 Passot S, Couvreur V, Meunier F, et al (2018) Connecting the dots between computational tools
564 to analyse soil-root water relations. Exp Bot

565 Polomsky J, Kuhn N (2002) Root Research Methods. In: Tom Beeckman UKYWAE (ed) Plant
566 Roots: The Hidden Half, third. CRC Press, pp 447–487

567 Riley D, Barber SA (1970) Salt accumulation at the soybean (GLYCINE MAX. (L.) MERR.) root-soil
568 interface. Soil Sci Soc Am J 34:154–155

569 Schröder N, Lazarovitch N, Vanderborght J, et al (2014) Linking transpiration reduction to
570 rhizosphere salinity using a 3D coupled soil-plant model. Plant Soil 377:277–293
571 Schröder N, Lazarovitch N, Vanderborght J, et al (2013) Linking transpiration reduction to
572 rhizosphere salinity using a 3D coupled soil-plant model. Plant Soil 377:277–293
573 Sinha B.K. and Singh N.T (1976) Salt Distribution Around Roots of Wheat Under Different
574 Transpiration Rates. Plant Soil 44:141–147
575 Stebbins RL, Dewey DH (1972) Role of transpiration and phloem transport in accumulation of
576 45calcium in leaves of young apple trees. Amer Soc Hort Sci J
577 van Genuchten MT (1980) A Closed-form Equation for Predicting the Hydraulic Conductivity of
578 Unsaturated Soils1. Soil Sci Soc Am J 44:892. doi:
579 10.2136/sssaj1980.03615995004400050002x
580 Warren JM, Meinzer FC, Brooks JR, et al (2007) Hydraulic redistribution of soil water in two old-
581 growth coniferous forests: Quantifying patterns and controls. New Phytol 173:753–765.
582 doi: 10.1111/j.1469-8137.2006.01963.x
583 Wohlfahrt G, Bianchi K, Cernusca A (2006) Leaf and stem maximum water storage capacity of
584 herbaceous plants in a mountain meadow. J Hydrol 319:383–390
585 Yang J, Kloepper JW, Ryu CM (2009) Rhizosphere bacteria help plants tolerate abiotic stress.
586 Trends Plant Sci 14:1–4
587

588 *List of figures*

589 *Figure 1:* Tomato plant growing on a Rhizoslide. The plant (A) is placed on the paper sheet 10X14 cm (B),
590 inside a sealed plastic bag (C), so water can be only transpired. Irrigation is applied through a small cut in
591 the plastic bag (D) with a pipette, without contact with the paper. Na^+ concentration was sampled from
592 discs (0.7 cm diameter), in growing distance from the root; (1) -0.35-0.35 cm, (2) 0.35-1.05 cm and (3)
593 1.05-1.75 cm (E). The bags are placed in a box to keep the roots in the dark.

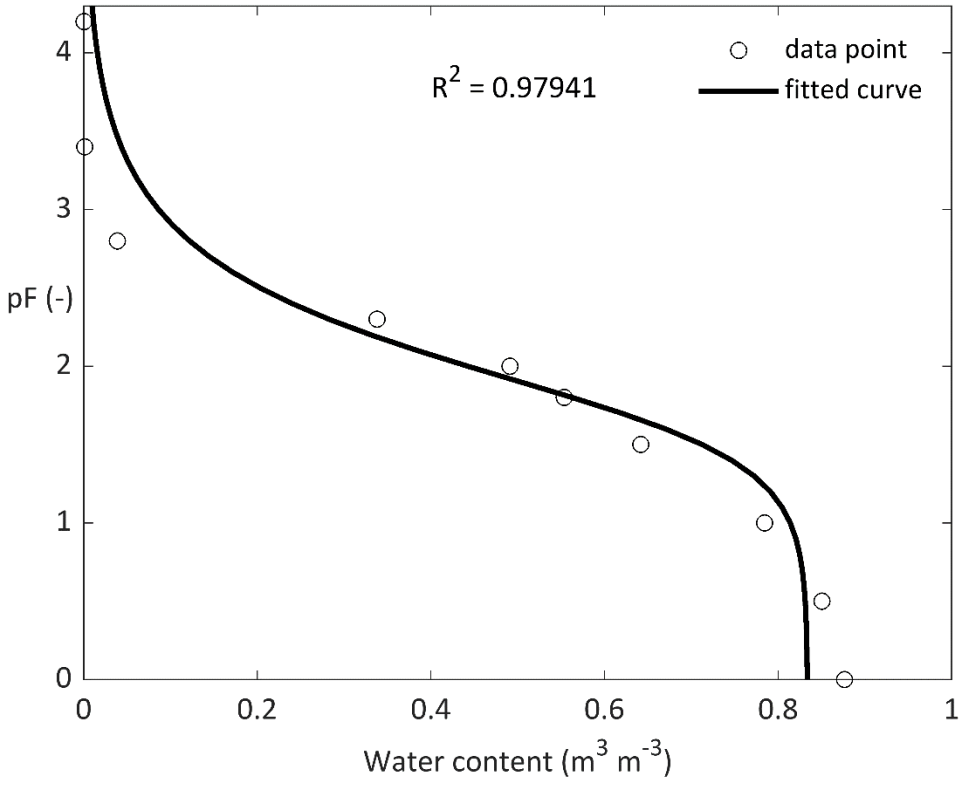

Figure 2: Water retention curve of filter paper used in the rhizoslide setup. Experimental data is represented by dots, while the fitted curve to the van Genuchten function is represented by a thick black line. Obtained values for the van Genuchten parameters were θ_s = 0.83396, θ_r = 0.001, α = 0.01982 cm^{-1} and n = 1.7622.

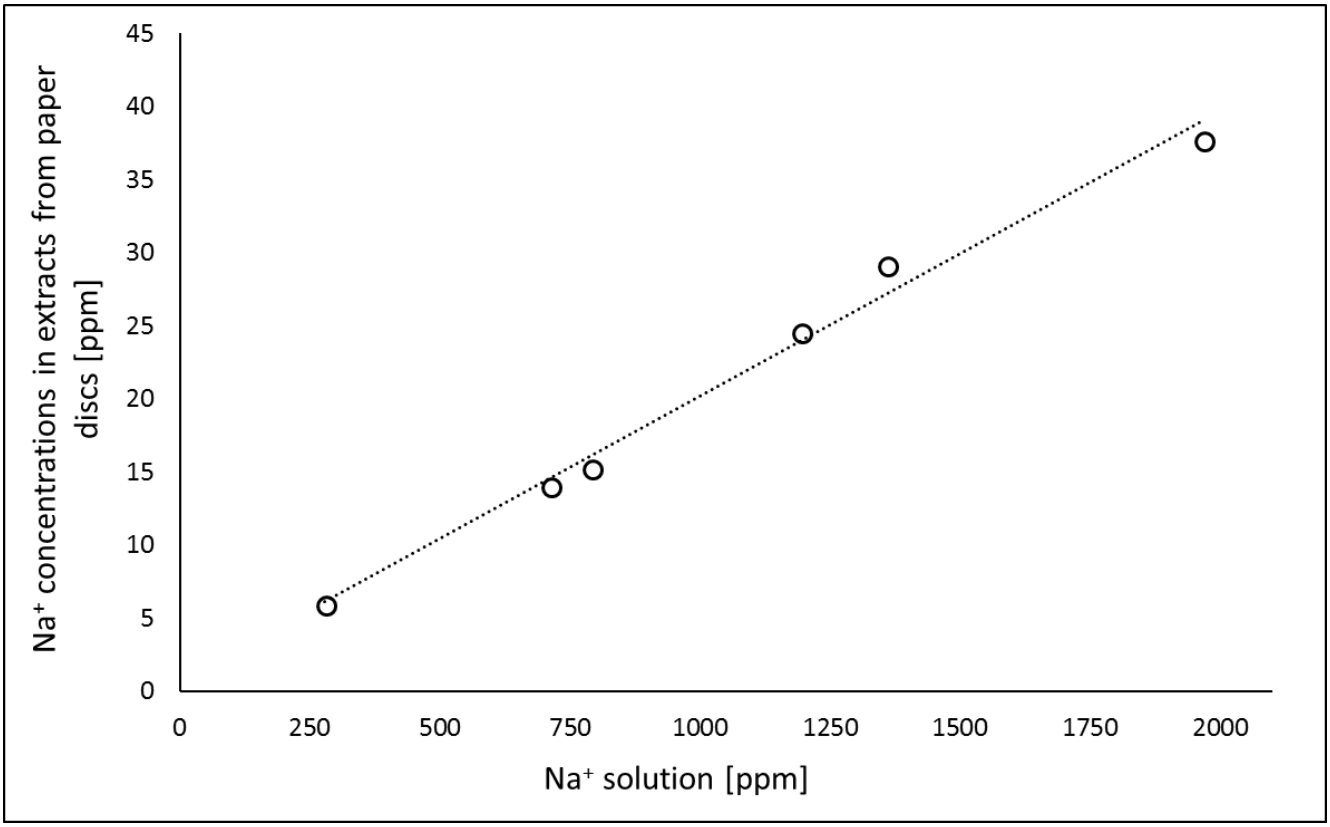

599

600 *Figure 3:* Calibration curve between Na^+ concentrations in the solution the rhizoslides were dipped in
601 and the concentration found in the extracts of the cutout discs. Each dot represents an average value of
602 three measurements. $y = 0.0195x + 0.7241$, $R^2 = 0.9893$.

603

604

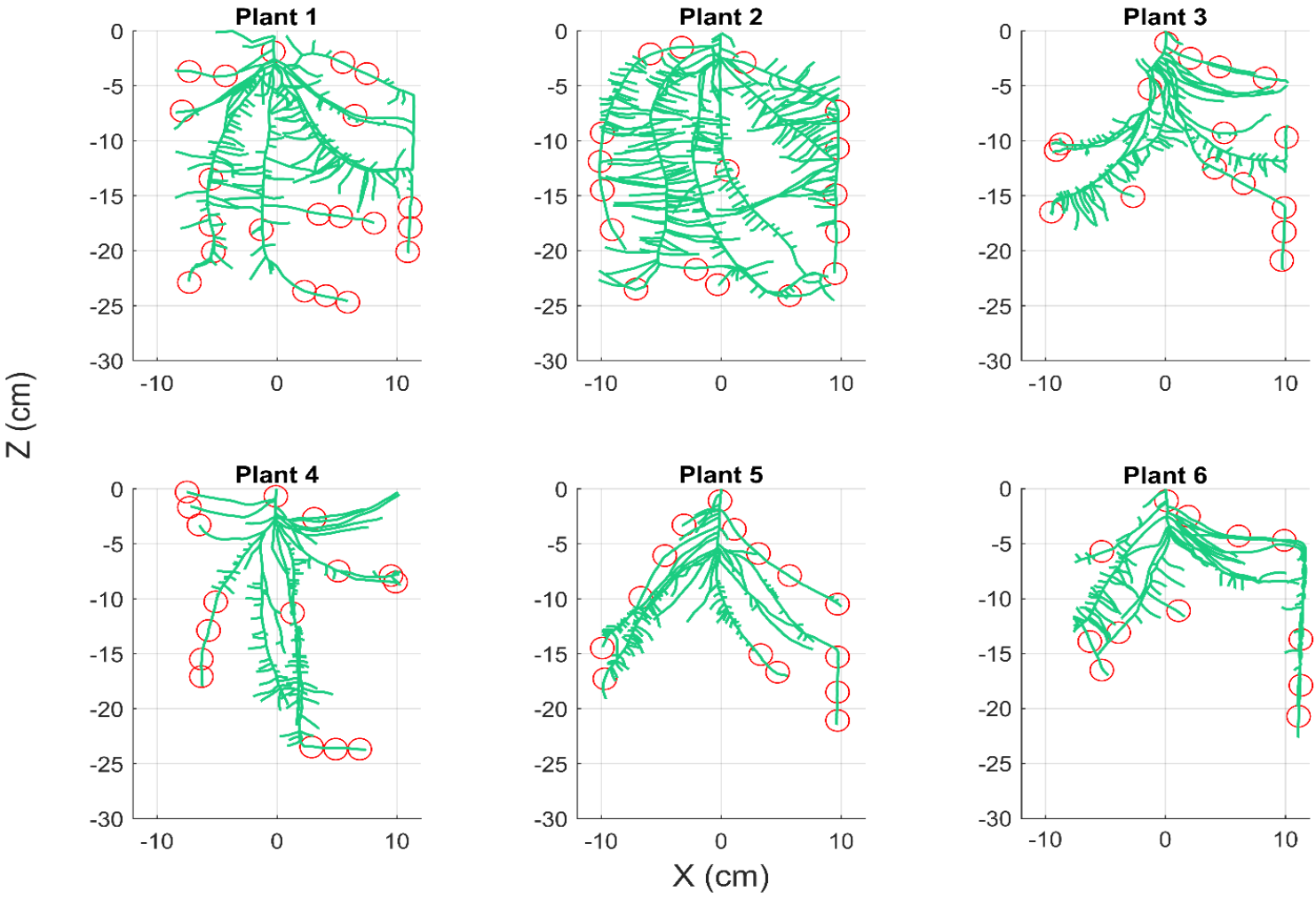

605 *Figure 4:* Schematic representation of the 6 root systems studied in the simulation part of this study. The
606 red circles represent the sampling points at which simulated salt concentration gradients from the soil-
607 root interface to the bulk soil were measured.

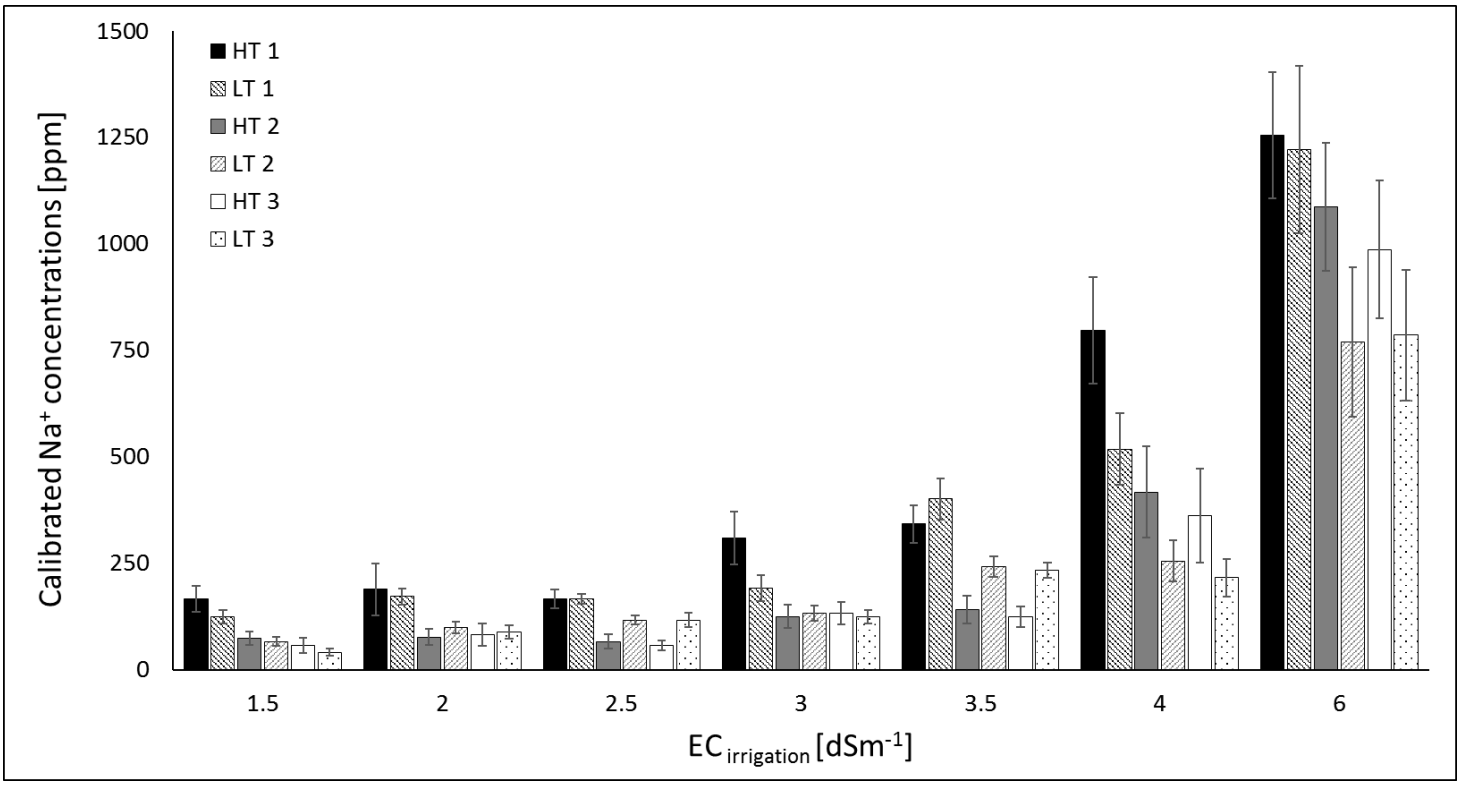

608 *Figure 5:* Effect of salinity level of the irrigation water, transpiration rate and distance from the root on
609 Na^+ concentrations. Results of measurements in growing distance from the root: -0.35-0.35 cm (dist 1),
610 0.35-1.05 cm (dist 2) and 1.05-1.75 cm (dist 3), under two transpiration rates: low (60%) and high
611 (100%).

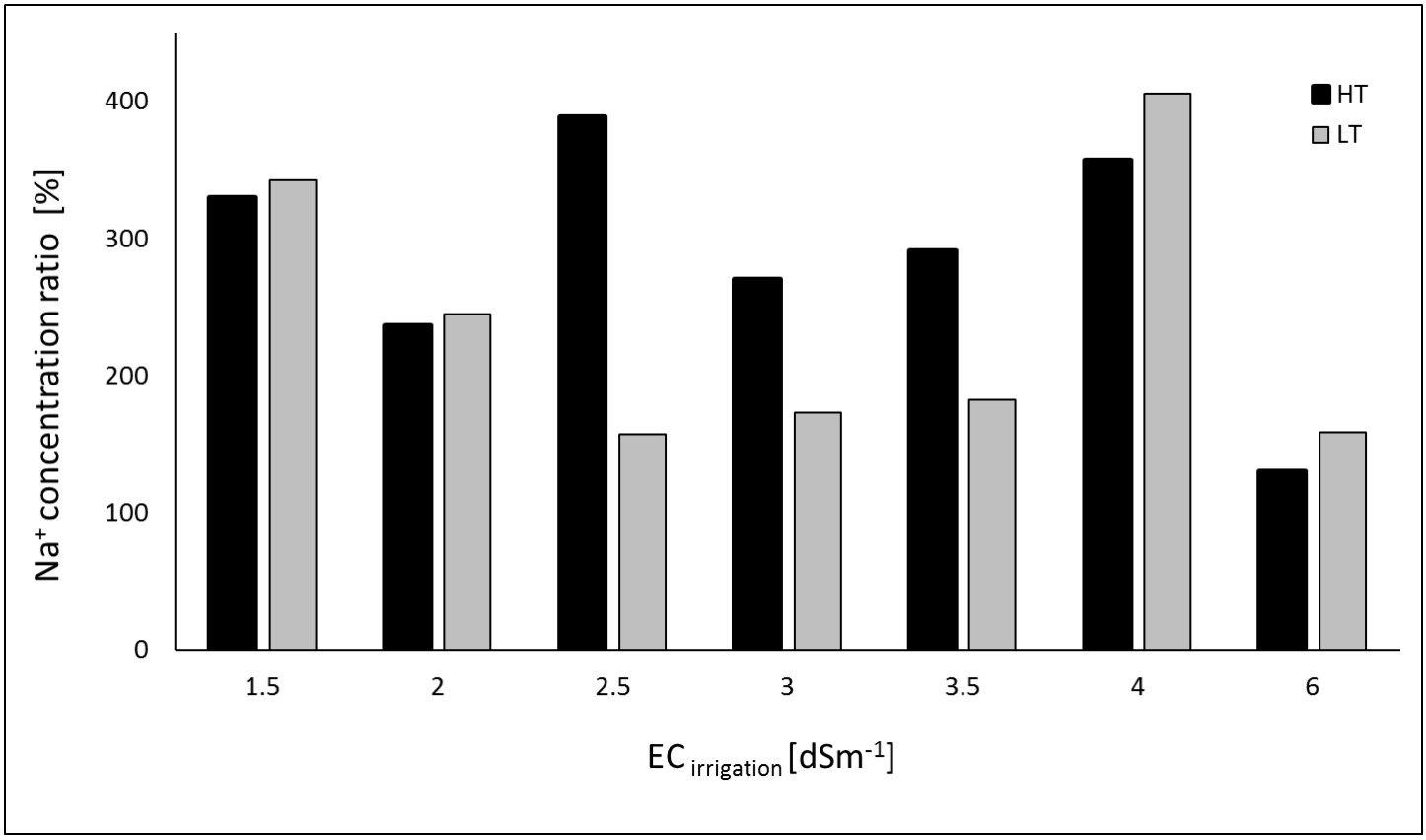

612

613 *Figure 6:* Na^+ concentration ratio of closest distance (dist 1) to furthest distance (dist 3), found in the
614 cut-out discs (Equation 1) under two transpiration rates and various salinity levels.

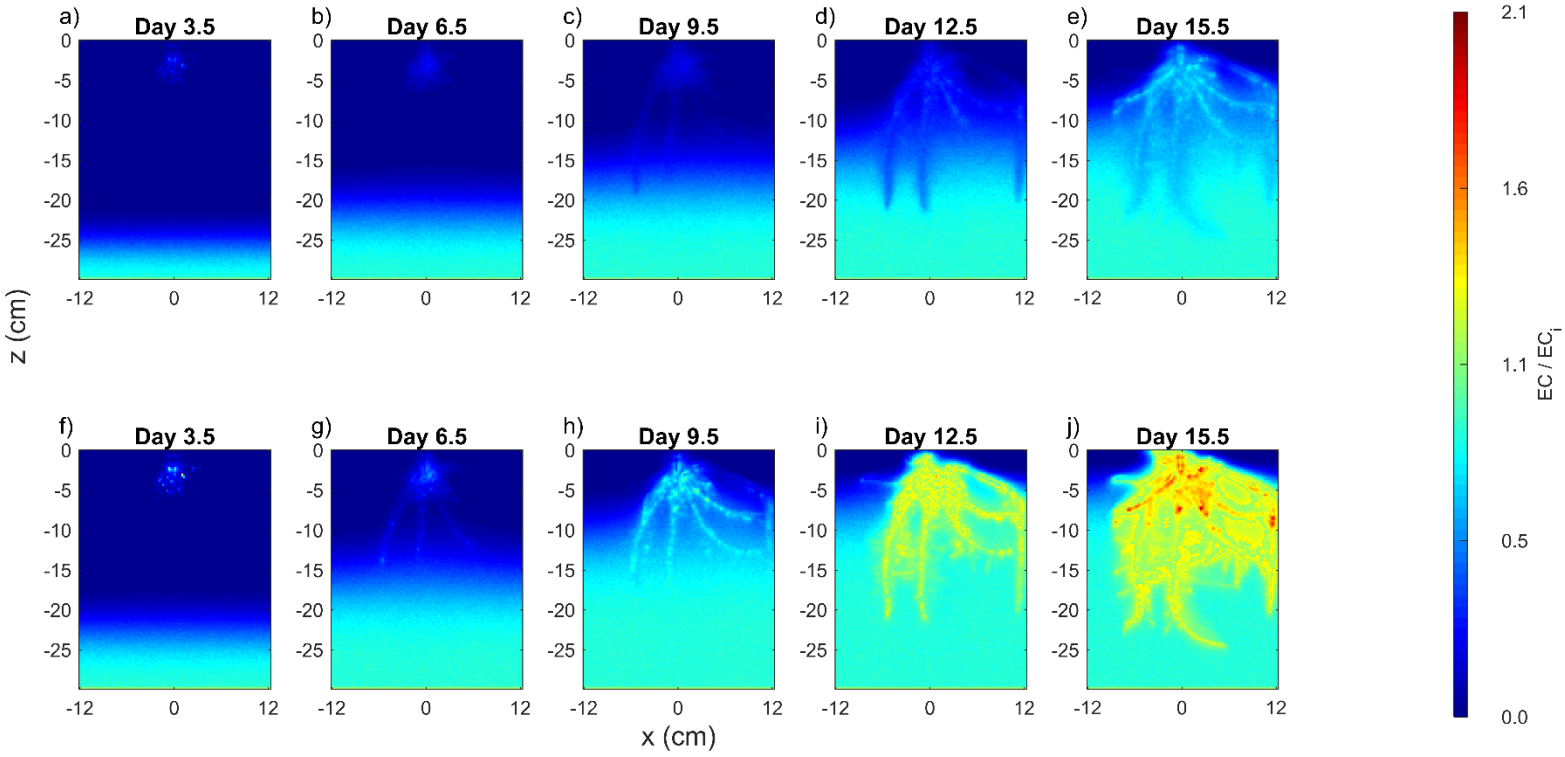

616 *Figure 7*: Salt relative concentration (EC/EC_i, EC_i is EC in irrigation water) results for simulations
617 performed on Plant 1 with EC = 4 dS m^{-1} in the irrigation water. Plots a, b, c, d and e correspond to the
618 low transpiration rate, whereas f, g, h, i and j depict the high transpiration rate. .

619

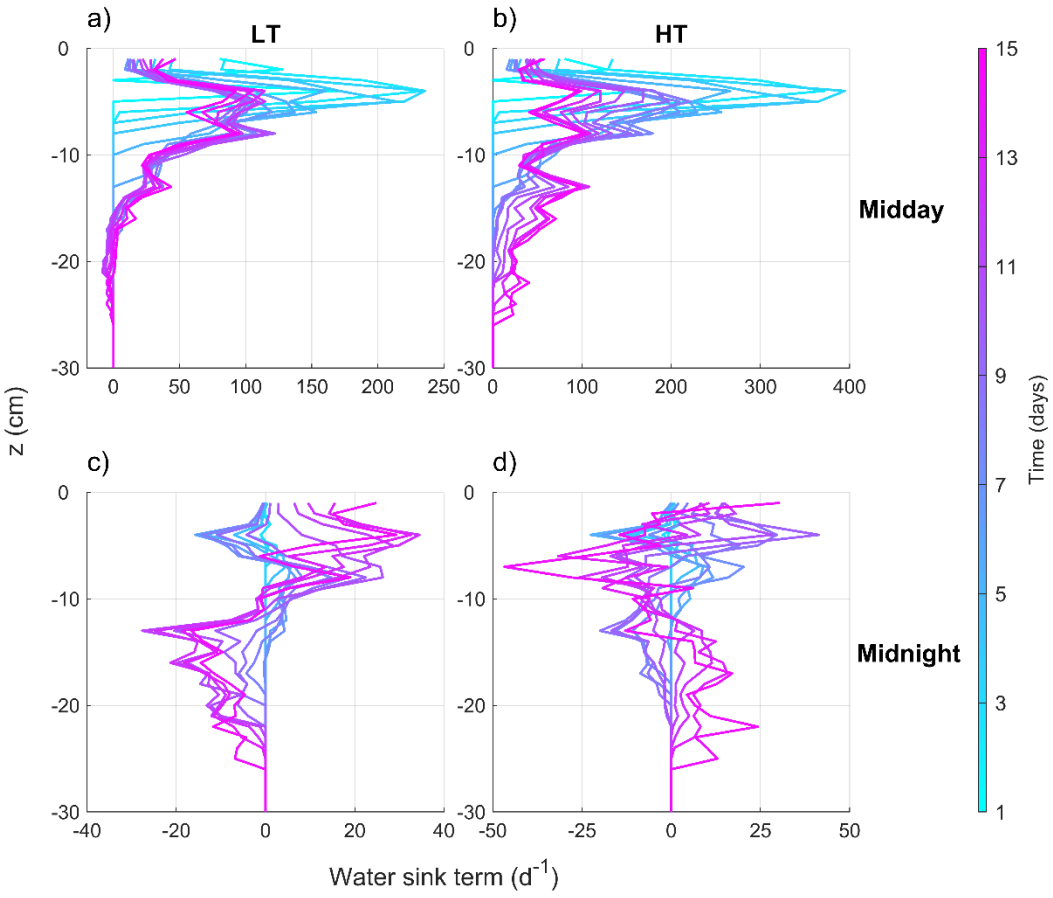

620

621 *Figure 8*: Water sink (cm^3 of water taken up per cm^3 of 'soil' per day) distribution per depth with time for
622 simulation performed on Plant 1 with EC = 4 dS m^{-1} in the irrigation water. Upper plots (a and b) present
623 data obtained during midday and lower plots (c and d) present midnight data. Left plots (a and c)
624 present data under LT whereas right plots (b and d) present HT data.

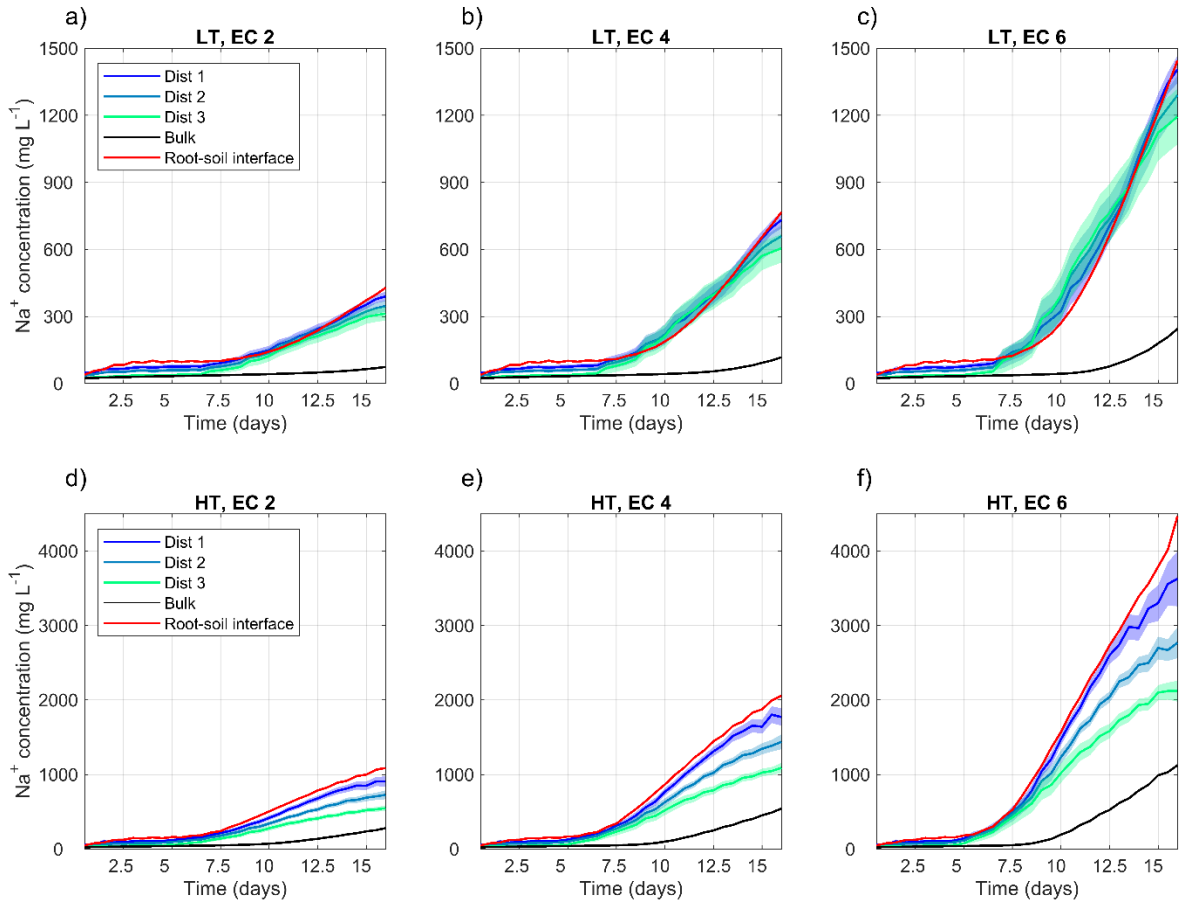

625

626 *Figure 9:* Temporal change in simulated salt concentration in the bulk (black), root-soil interface (red)
627 and at different distances from the root surface: 0.4 – 0.4 cm (dist 1), 0.4 – 1.0 cm (dist 2) and 1.0 – 1.8
628 cm (dist 3). Solid lines represent mean solute concentration, whereas shaded areas represent
629 concentration values compressed between mean ± SEM (n=21). The plotted mean concentrations are
630 the average of all plants in all sampled points. Plots a, b and c correspond to low transpiration treatment
631 simulations (LT), whereas d, e and f relate to simulations under high transpiration demand (HT).

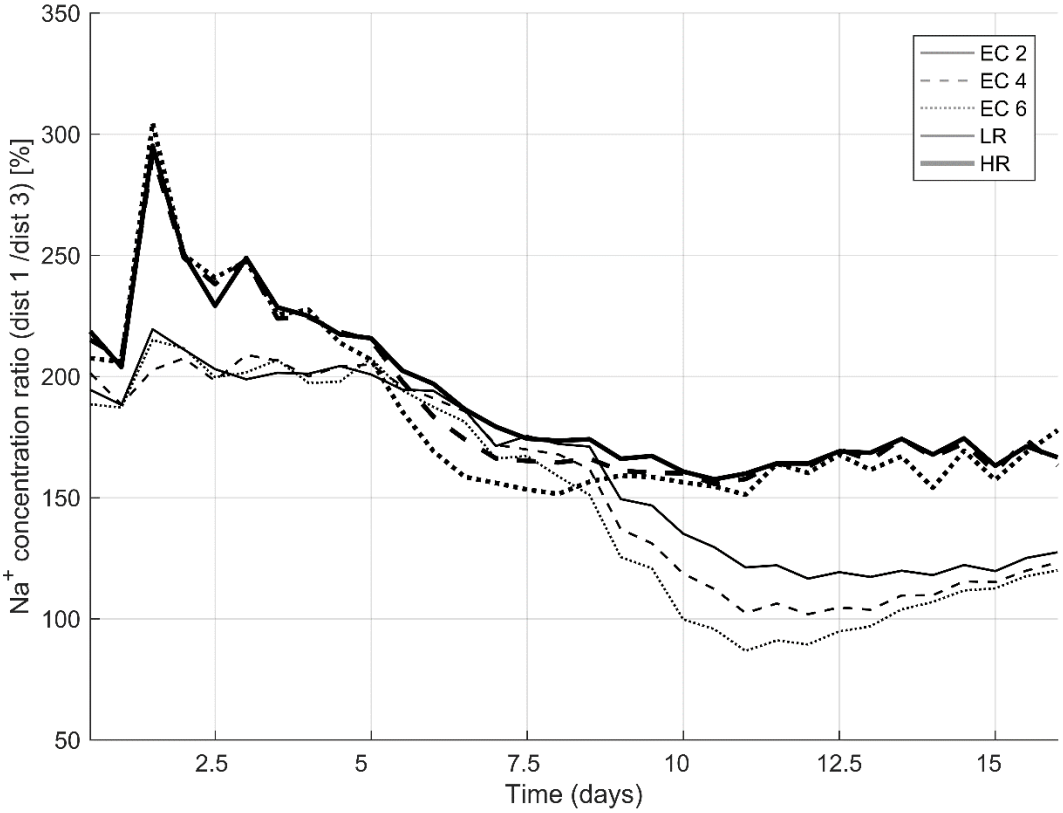

Figure 10: Temporal change in simulated Na^+ concentration ratio of closest distance (dist 1) to furthest distance (dist3) under low and high rate transpiration, and different salinity levels.

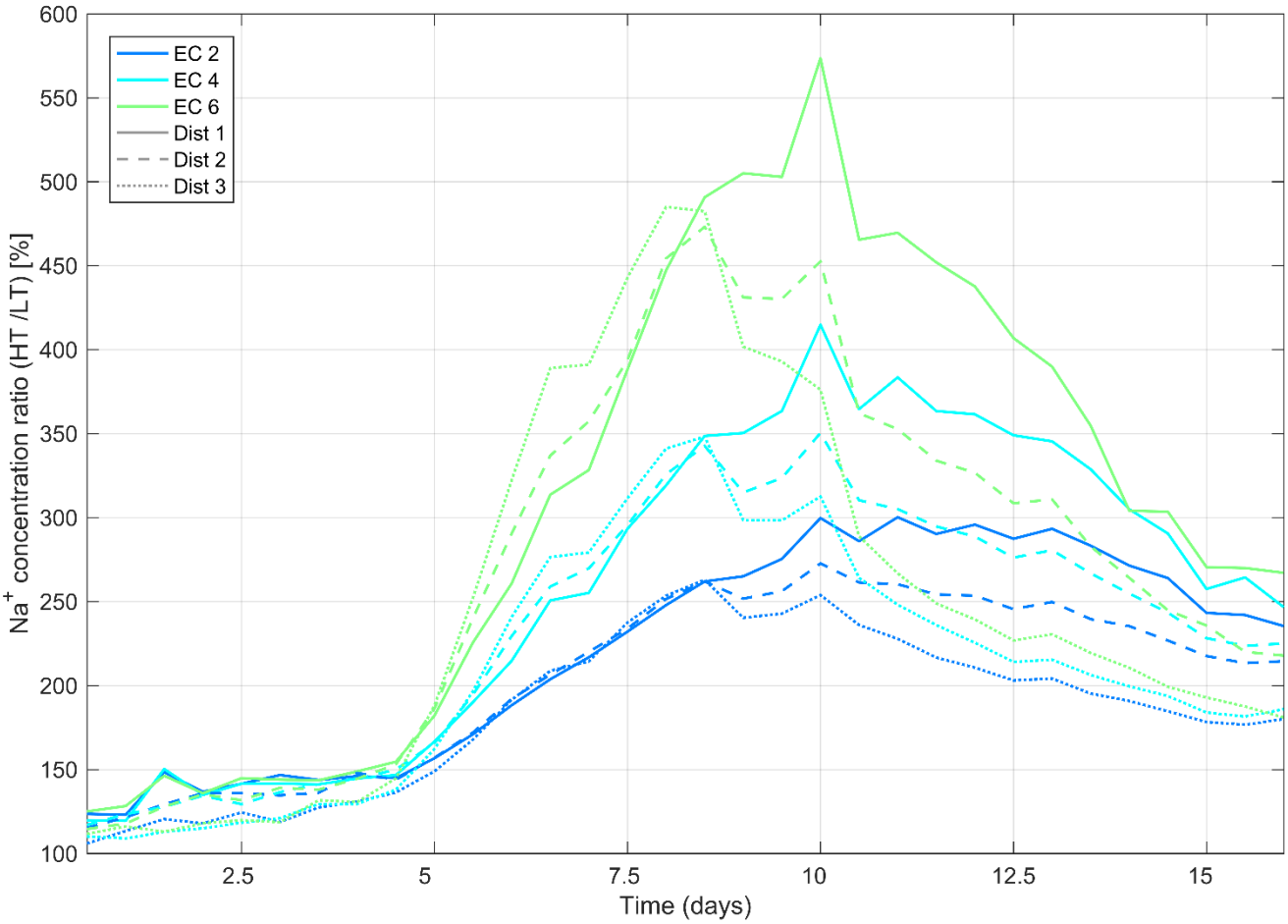

635 *Figure 11:* Temporal change in simulated Na^+ concentration ratio of high transpiration to low
636 transpiration at different distances from the root surface: 0.4 – 0.4 cm (dist 1), 0.4 – 1.0 cm (dist 2) and
637 1.0 – 1.8 cm (dist 3).

638

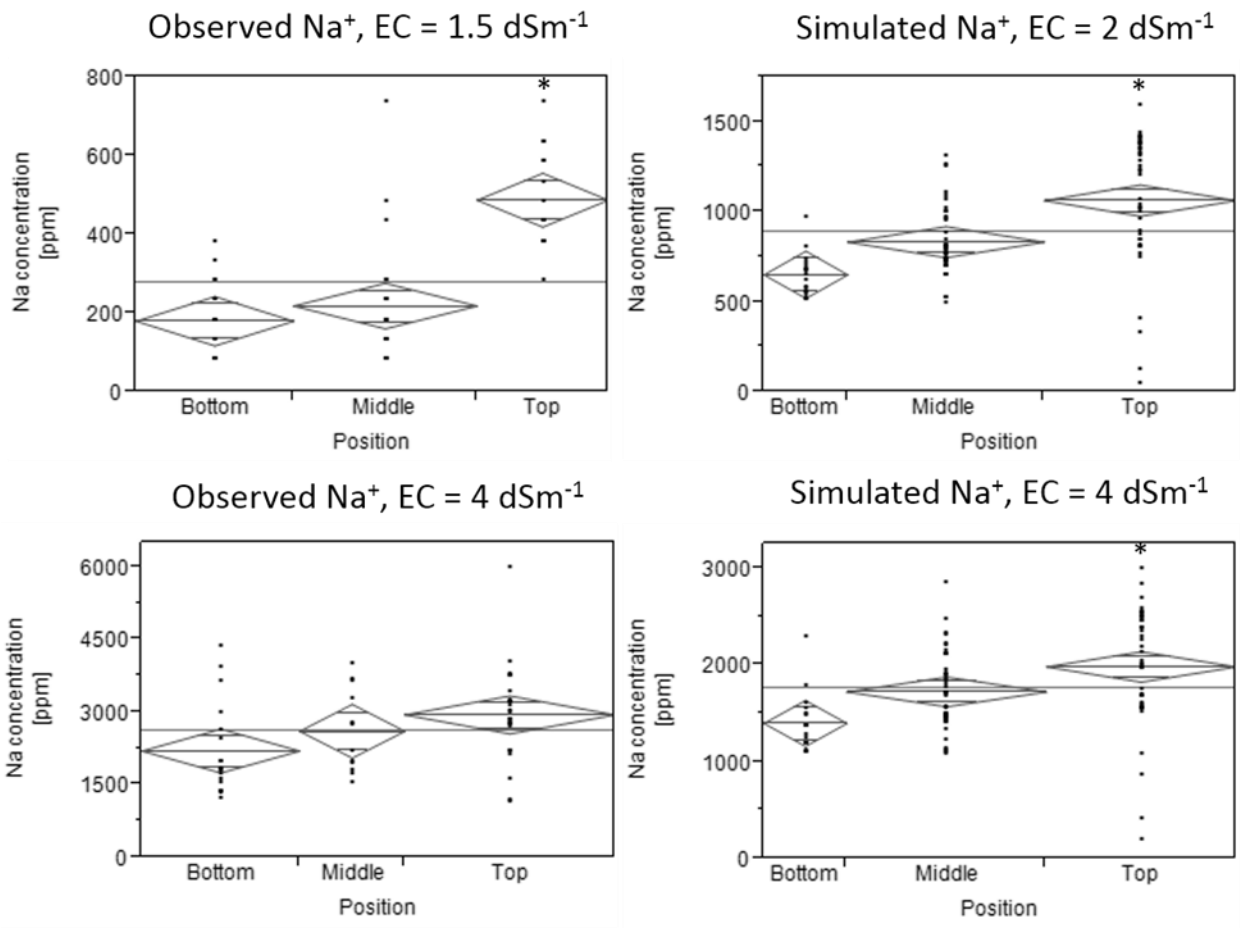

639

640 *Figure 12*: Observed and simulated Na^+ concentrations at dist 1 (closest to the root) at different
641 positions of the rhizoslide, under two salinity levels. Comparison was done with Tukey - Kramer test, *
642 represent a significant difference, $\alpha = 0.05$.

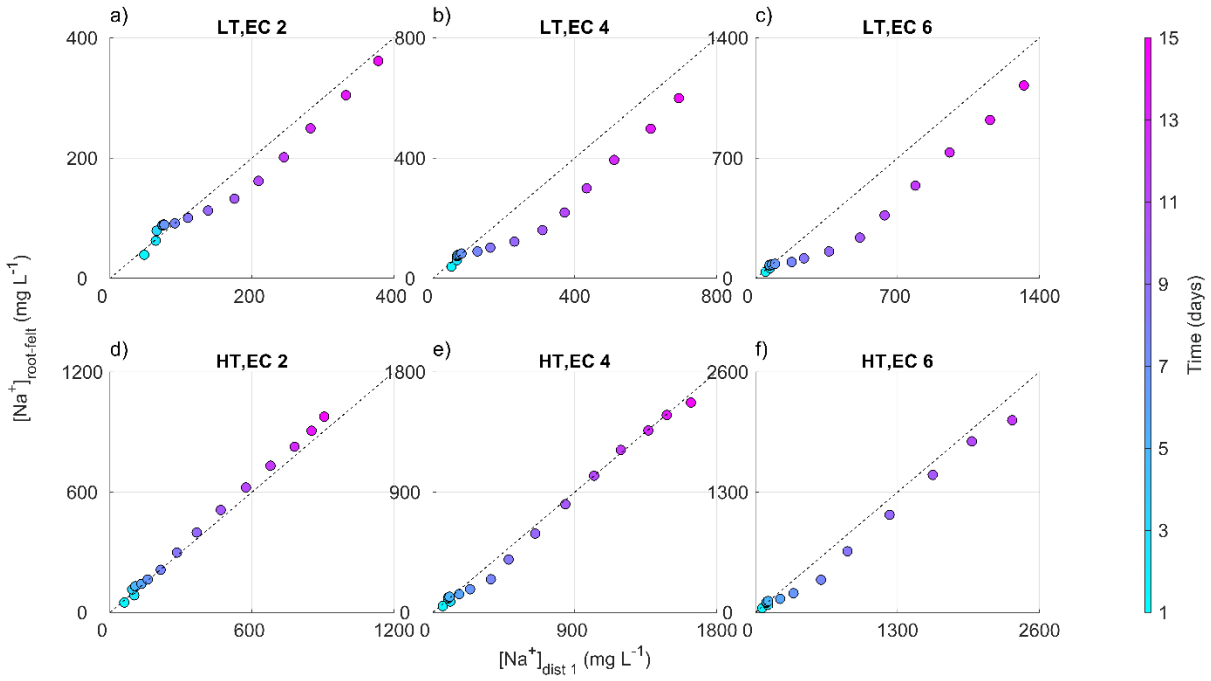

Figure 13: Comparison between bulk soil and root felt Na^+ concentrations (mg L^{-1}) at midday.

List of tables

Table 1: leaves mass and total plant mass (FM: fresh mass) between each transpiration rate at each salinity level were compared. Different letters represent significant differences. Average transpiration rate was calculated as the amount of transpired water during the time of the experiment divided by days of experiment. Comparison was done by using Student's T test (α = 0.05, n = 6 for each treatment combination).

EC [dS m^{-1}]	Transpiration treatment	Average transpiration rate [mL/day]	Std Dev	Leaves FM [g/plant]	Std Dev	Total FM [g/plant]	Std Dev
1.5	LT	3.6^{B}	± 0.3	2.42^{A}	± 0.57	5.24^{B}	± 0.8
	HT	5.5^{A}	± 0.2	2.96^{A}	± 0.74	6.5^{A}	± 0.68
4	LT	3.8^{B}	± 0.3	2.36^{B}	± 0.51	4.97^{B}	± 0.73
	HT	5.2^{A}	± 0.6	3.37^{A}	± 0.91	7.03^{A}	± 1.39